

Synthesis, characterization, and removal of fluoride and chromium by Chitosan based Graphene Oxide Nanocomposite

Bharti¹, Dr. Manish Srivastava², Dr. Anamika Srivastava³

¹Department of Earth Sciences, Banasthali Vidyapeeth, Newai (Rajasthan)

²Department of Chemistry, Central University, Allahabad

³Department of Chemistry, Banasthali Vidyapeeth, Newai (Rajasthan)

Corresponding author mail id: bhartimehla22@gmail.com

Abstract

Objective: The objective of this study was to examine the adsorption properties of fluoride and chromium using a recently synthesised nanocomposite of graphene oxide-chitosan (GO-Ch-NC) and graphene oxide (GO) nanoparticles.

Methodology: The synthesis and evaluation of the GO nanoparticle and GO-Ch-NC were conducted utilizing several analytical methods, such as Scanning electron microscopy (SEM), Fourier-transform infrared spectroscopy (FTIR), and X-ray diffraction. Following this, a sequence of tests was undertaken to examine the alterations in the adsorption capacity of fluoride and chromium based on variations in the concentration of the adsorbent, pH levels, and temperature. The results acquired from the adsorption investigations conducted with GO-Ch-NC were subjected to analysis utilizing the Langmuir and Freundlich equations.

Result: The laboratory studies yielded findings indicating that the particle size of the graphene oxide-chitosan nanocomposite was determined to be 250 μm . The Freundlich isotherm was determined to be a suitable model for describing equilibrium data of Cr (VI) and F ion adsorption. The kinetics of adsorption may be described using rate expression that follows a pseudo-second-order model. The successful elimination of fluoride and chromium (VI) ions was reported to occur at pH levels of 5 and 7, respectively. The study determined that the highest level of elimination achieved was 55% for fluoride and 80% for chromium (VI) ions.

Conclusion: The experimental findings indicated that the synthesized materials have shown significant capability in removing fluoride and Cr (VI) ions from aqueous solutions. The fascinating prospect of future generations developing adsorbents that exhibit both great efficiency and cost-effectiveness is evident.

Keywords: Adsorbents, Chromium, Graphene Oxide, Nanoparticles, Nanocomposites

1. Introduction

The issue of fluoride contamination in water environments, resulting from both natural and anthropogenic activity, has gained global recognition as a significant concern [1]. The development of efficient and resilient technology for removal of excess fluoride from water environments is of utmost importance [2].

The proliferation of industrialization and the emergence of modern technology in emerging nations have led to a significant increase in water pollution, so posing a substantial risk to the environment, human well-being, and economic stability [3, 4]. While some metals are essential for human dietary needs in small quantities, their excessive presence in the environment is linked to significant issues [5, 6]. The issue of water pollution is increasing globally because of the prevalence of many toxins, including arsenic, fluoride, and chromium [7]. The issue of water contamination has gained increasing significance in recent years, mostly owing to the adverse impacts on human health associated with the presence of dissolved ions and heavy metals [8].

The literature often reports the presence of many pollutants in water, including arsenite, arsenate, chromium, copper, fluoride & mercury. The principal pollutants in water, arising from both natural and human activity, are As (III), As (V), F⁻, & Cr (VI) [9]. The occurrence of these pollutants may be attributed to either natural or manmade phenomena. The compound in question can induce carcinogenic and mutagenesis effects, hence posing a significant risk to many forms of life [10]. Consequently, the effective elimination of Cr (VI) and F⁻ prior to its release into the surrounding environment has emerged as a crucial concern from both biological and environmental standpoints [11].

The issue has prompted the investigation of approaches aimed at exploring and advancing technology for the purpose of eliminating harmful toxins from water sources [12]. There are several approaches to address the treatment of chromium and fluoride in industrial effluents; nevertheless, these systems encounter significant challenges including costliness, maintenance requirements, concerns over fossil fuel preservation, and unsanitary waiting times [13]. Adsorption is a widely used method in many applications owing to its adaptability, significant adsorption capacity, & cost-effectiveness [14]. The adsorption approach is often used for the removal of fluoride and has been extensively studied as a treatment technology. This method is known for its effectiveness, simplicity, and cost-effectiveness in removing fluoride from water [15]. Various adsorbents have been used for removal of fluoride and chromium from the water. Research indicated that polypyrrole homopolymer exhibits a higher number of active sites, hence establishing its potential as an effective adsorbent for the elimination of fluoride [16]. Electrospun alumina nanofibers have also been shown to have a high adsorption capacity of Chromium (VI) levels of fluoride concentrations of 1.2 mg/g and 7.9 mg/g [17].

In this study, we aimed to synthesize 2 adsorbents, Graphene oxide (GO) nanoparticles and Graphene oxide-chitosan nanocomposites, to evaluate their efficacy in removing fluoride and chromium in wastewater.

2. Methodology

2.1 Materials

The low molecular weight Chitosan was procured from Sigma Aldrich. Fine Chem Ltd., a company based in Mumbai, India, supplied many chemical compounds, including graphene oxide, chitosan, sodium borohydride, potassium permanganate, sodium nitrate. Graphene oxide, Graphene oxide Chitosan composite were obtained from pharmaceutical establishments. Deionized water was used for all experimental procedures.

2.2 Synthesis of adsorbents

Synthesis of GO Nanoparticles (GO-Np) - The experiment included the combination of 3g of graphite flakes with 3g of Sodium Nitrate, followed by stirring. Subsequently, 138 ml of sulphuric acid (SO₄) (was added to mixture, & then placed in an ice bath for a duration of 30 minutes. An amount of 18g of potassium permanganate was introduced into the solution. The sample was subjected to the temp. of 35°C for a day, by the adding of 240ml of water. Subsequently, Sodium borohydride was introduced into the solution containing Graphene oxide. The observation of a change in hue to black indicated the development of graphene oxide nanoparticles (GO NPs). The sample was subjected to centrifugation at a speed of 10,000 revolutions per minute (rpm) to separate the pellet. The resulting pellet was then subjected to washing with acid and base solutions for a duration of 30 minutes each.

Synthesis of GO-Chitosan nanocomposite (GO-Ch NC)—The nanoparticles of graphene oxide (GO) were distributed into a solution of chitosan. The solution underwent heating while being subjected to ultrasonic vibration. Subsequently, the solution was subjected to centrifugation. The specimen was subjected to a cleaning process including deionized water followed by drying under vacuum conditions. The formation of the polymer nanocomposite occurred.

2.3 Characterization of the synthesized adsorbents

Prior to using adsorbents for further investigations, a range of procedures was used to characterize the adsorbent, as outlined below—

- **Fourier transforms infrared spectroscopy (FTIR)**—FTIR measurements of synthesized nanocomposites were conducted using a Perkin Elmer UATR Two FTIR spectrophotometer within the spectral region of 400-4000 cm⁻¹.
- **XRD (X-Ray Diffraction):** -The degree of crystallinity shown by GO-Ch NC and GO was assessed using ADX2700 rotating X-ray diffractometer within 3θ range of 13-85 degrees. The X-ray diffractometer was used to assess crystallinity and interlayer modifications in GO-Ch NC particles.

- **SEM (Scanning electron microscopy)/ EDX:** - The crystalline structures and elemental analyses of GO-Ch NC and GO were examined using an SEM equipped with an electron dispersive X-ray spectrometer (EDX) (FESEM MIRA3 TESCAN).

2.4 Batch adsorption study

Dissolving a fixed quantity of Merck $K_2Cr_2O_7$ & NaF in deionized water yielded a 1000 milligram/L stock solution of and Cr (VI) ions. The stock solution was diluted to reach the desired fluoride concentrations and chromium (VI). Various amounts of nano adsorbents (10-100 mg) were added to a 20 mL solution with fluoride and chromium (VI) for batch adsorption testing. The test solution and adsorbents were placed in flasks and shaken at 150 rpm at 30 °C. This research examined how pH affects fluoride and Cr (VI) ion adsorption by nano adsorbents. By mixing 0.1 M NH_4OH and 0.1 M HNO_3 , the pH of the mixture was changed from 3 to 9. Similar research examined how adsorbent dose affected Cr (VI) and fluoride ion adsorption. A 20 mL solution with 10 mg/L concentration was agitated for 1 hour to accomplish this. Adsorbent doses ranged from 0.01 to 0.3 g at ambient temperature. After equilibrium, Whatman filter paper separated the adsorbent from the aqueous solution. Atomic Absorption Spectroscopy (AAS) & an Orion ion-selective electrode were used to measure the leftover metal ion concentrations. The test solution and adsorbents were put in flasks and stirred with a 150-rpm mechanical shaker at 30 °C. This study evaluated how pH affects Cr (VI) and fluoride ion adsorption on nano adsorbents.

The pH of the solution was consistently regulated within the pH range of 3 to 9 by using an aqueous solution consisting of 0.2 M NH_4OH and 0.4 M HNO_3 . Furthermore, a research investigation was conducted to investigate the impact of varying dosages on the adsorption actions of chromium (VI) and fluoride ions. The experiment included stirring a 20 mL solution with a stock concentration of 10 mg/L for a length of 1 hour, using different quantities of adsorbent doses ranging from 0.01 to 0.1 grammes, all conducted at ambient temperature. After achieving equilibrium, the adsorbent material was separated from the aqueous solution by the filtration process, employing Whatman-42 filter paper. Subsequently, the remaining concentrations of the metal ions in the extracted portion were ascertained using Atomic Absorption Spectroscopy (AAS) and an Orion ion-selective electrode.

The adsorption data acquired during this experimental investigation were assessed using the Freundlich and Langmuir isotherm models. The adsorption percentages of chromium (VI) and fluoride ions were calculated by subtracting the initial concentrations (C_i) from the final concentrations (C_f) of both ions in an aqueous solution, both before and after contact.

$$\% \text{ removal} = \frac{C_i - C_f}{C_i} \times 100$$

3. Result and Discussion

The aquatic environment has seen a notable deterioration in water quality over the last several decades, mostly attributed to the introduction of hazardous species because of human activities. Graphene oxide nanoparticles and Graphene oxide-chitosan nanocomposites were prepared and characterized.

3.1 Characterization of synthesized compound

A. FTIR

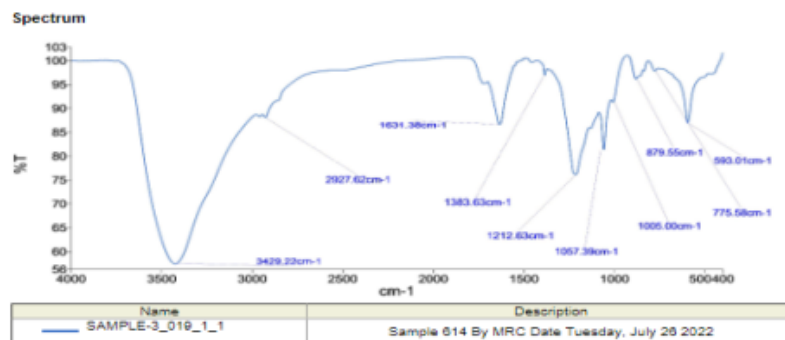


Figure 1. FTIR spectra of GO

FTIR spectroscopy was used to investigate existence of oxygen-containing functional groups that are indicative of Graphene oxide (GO). Figure 1. displays the FTIR spectra of graphene oxide (GO). The characteristic peaks seen in the generated graphene oxide (GO) were found at wavenumbers of 3429.22 cm⁻¹, 1631.36 cm⁻¹, 1212.63 cm⁻¹, 1057.39 cm⁻¹, 879.55 cm⁻¹, and 775.58 cm⁻¹. Previous studies have provided evidence indicating that vibrations associated with the elongation of the hydroxyl group exhibit a wide and intense peak at about 3500 cm⁻¹. The low-frequency area in proximity exhibited peaks at 2927.62 cm⁻¹, 1383.63 cm⁻¹, 1005.00 cm⁻¹, and 775.58 cm⁻¹.

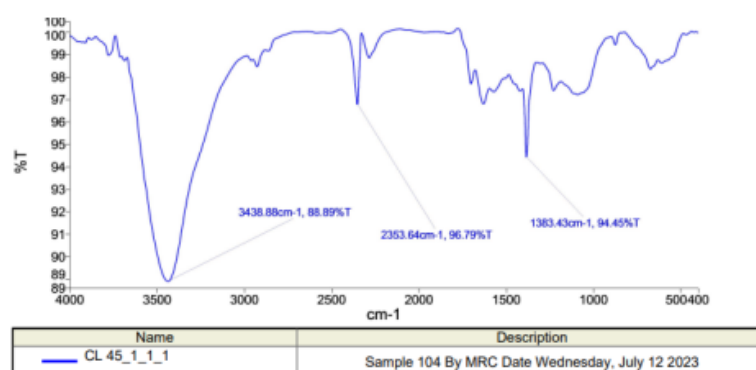


Figure 2. FTIR spectra of GO-Ch

FTIR spectra was used to investigate the existence of O₂-containing functional groups in GO-Ch. Figure 2 displays FTIR spectra of GO-Ch which were created for F and Cr removal using polymer adsorbents. The greatest peaks of GO-Ch peak were observed, at 3438.88 cm⁻¹. Two smaller peaks were detected at 2353.64cm⁻¹, 1383.43cm⁻¹. It is demonstrated that stretching vibrations of OH groups, which may be triggered by absorbed H₂O molecules, phenolic OH, or OH from carboxylic groups, form a wide and potent peak in the range of 3700 to 3000 cm⁻¹.

B. XRD

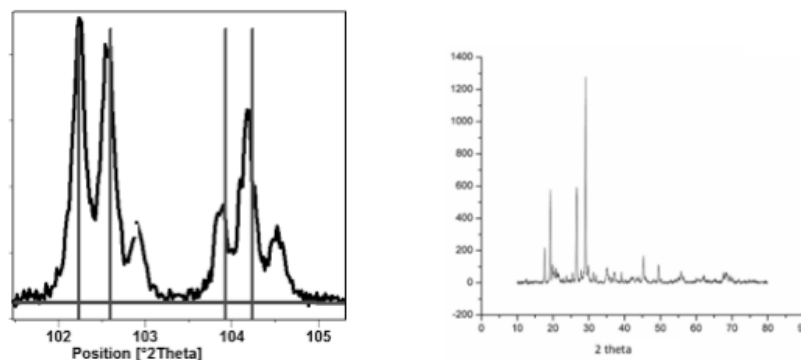
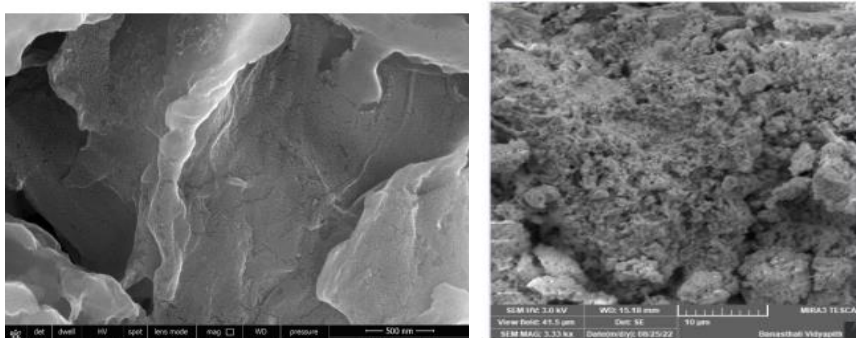


Figure 3. XRD Analysis of 1) GO Np and 2) GO-Ch-NC

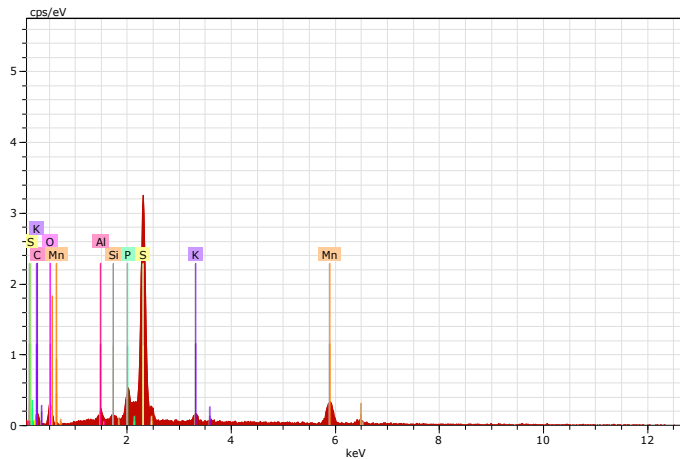
The XRD method is widely utilized for crystal identification & has emerged as a significant area of study within the scientific community in recent years. The GO XRD patterns are seen in Figure 3. XRD pattern exhibits evidence of the sample's crystalline structure. Figure 3. displays the XRD patterns of GO-Ch.

C. SEM



1)

2)



3)

Figure4. SEM Analysis of 1) GO Nanoparticles and 2) GO-Ch NC; 3) EDX of GO

Scanning electron microscopy image (figure 4. (1)) of graphene oxide (GO) showed a characteristic wrinkled and crumpled morphology, displaying uneven boundaries, rough topography, and evidence of scrolling-induced crumpling. The examination of the graphene oxide (GO) samples using scanning electron microscopy (SEM) indicated the presence of GO sheets of up to 10 μm in lateral dimensions, as well as smaller fragments measuring just a few microns in diameter. Figure 4(2) shows a scanning electron micrograph that illustrates the surface morphology of the GO chitosan composite nanoparticles. The experimental results provide evidence for the spherical morphology and homogeneous distribution of the synthesized composite nanoparticles consisting of graphene oxide and chitosan.

D) Raman Analysis

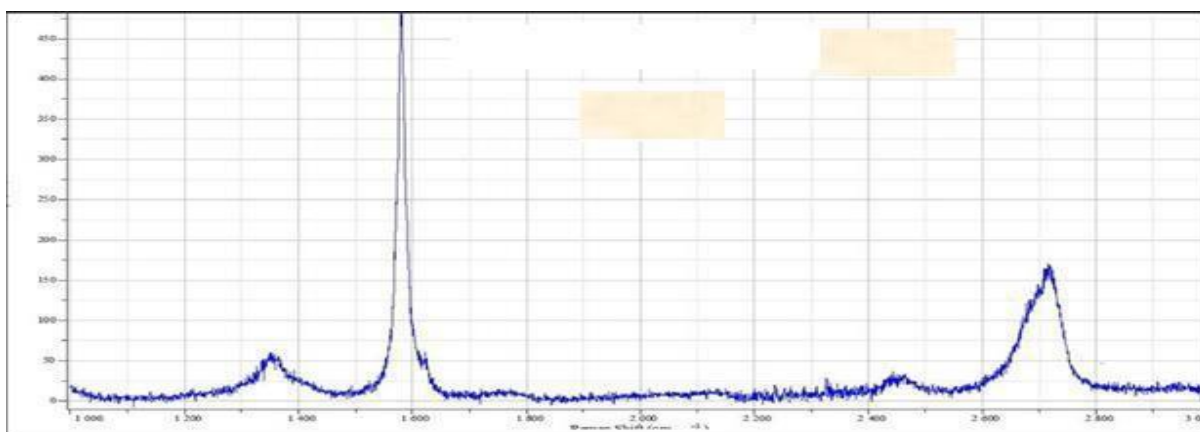


Figure 5. Raman Analysis of Graphene Oxide

Figure 5 depicts graphene oxide Raman analysis. Raman scattering is a helpful technique for characterizing graphite and graphene materials since it is substantially affected by their electrical structure. The Raman spectra of GO were found to be dramatically altered after the decrease. Raman spectroscopy is a popular method for characterizing carbon compounds because conjugated and double carbon-carbon bonds produce high Raman intensities. The substantial structural changes that occur during pristine graphite oxidation to GO. The virgin graphite Raman spectrum shows a pronounced G peak, which corresponds to the first-order scattering of the E_{2g} mode. The G band in GO is enlarged as a consequence of the decrease in size of the in-plane sp² domains. The decrease in the exfoliated GO might account for the smaller-than-average sp² domains by creating new graphitic domains that are more numerous than their larger-than-average predecessors in the GO.

4. Batch experiments

- **Effect of Adsorbent concentration on chromium adsorption capacity**

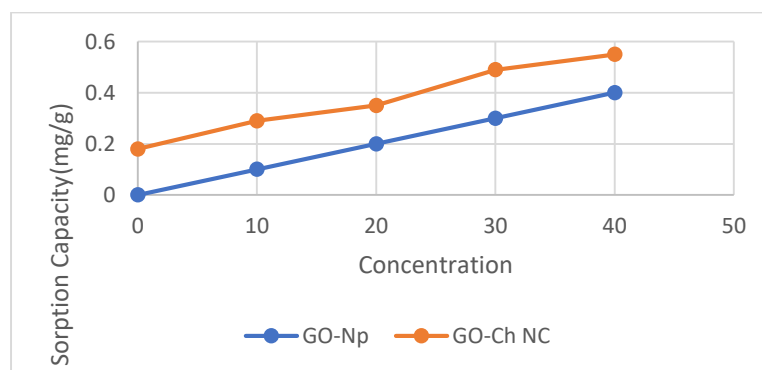


Figure 6. Effect of dosage of GO-Np and GO-Ch NC on adsorption capacity

The dose experiment optimised Cr (VI) elimination utilising GO nanoparticles and GO-Ch nanocomposites. Figure 6 shows the results of treating synthesised adsorbents at dosages of 0–40 g with 50 mL of 100 mg/L starting level. Adsorbent concentration improved chromium adsorption. Adsorption rises with adsorbent dose because surface area & sites increase. When dose surpassed 0.1 g, the synthesised adsorbent did not change. For future Cr (VI) absorption investigations, 0.1 g of adsorbent is optimal.

- **Effect of Adsorbent concentration on fluoride adsorption capacity**

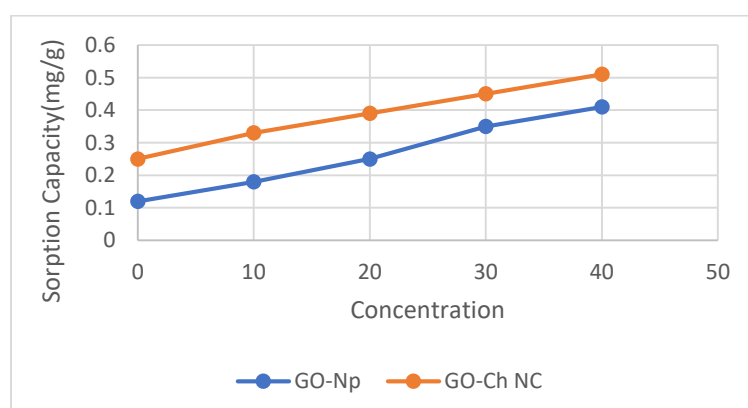


Figure 7. Effect of dosage of GO-Np and GO-Ch NC on adsorption capacity

The dosage experiments optimised GO nanoparticle and GO-Ch nanocomposites dose for fluoride elimination. Figure 7. shows increasing adsorbent concentration enhanced fluoride adsorption. Increasing adsorbent dose increases surface area and active sites, which enhances adsorption. When dosed over 0.1 g, the generated adsorbent did not change. Thus, for future fluoride sorption tests, 0.1 g of adsorbent is optimal.

- **Effect of pH on chromium adsorption capacity**

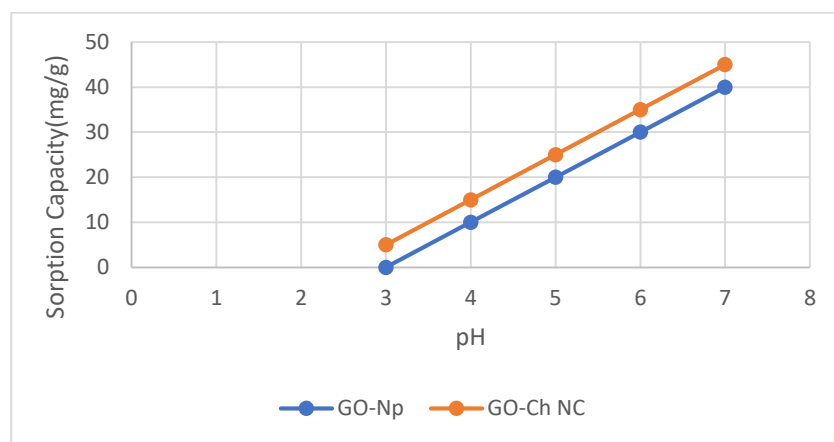


Figure 8. Absorption capacity of GO and GO-Ch NC at different pH

Chemically synthesised adsorbents were tested for chromium removal at various pH levels. Figure 8 demonstrates variation in adsorbent adsorption capacity by pH. Basic pH 10 inhibited chromium elimination, whereas pH 3 boosted it. Chromium species (HCrO_4^- , CrO_4^{2-} , and $\text{Cr}_2\text{O}_7^{2-}$) were diversely present at different pH levels. At low pH, GO and GO-Ch NC nanoparticles' protonated amine, carboxylic acid group, and higher potential metal ion increased adsorption ability. Thus, electrostatic attraction attracts negative charge chromium ions to the adsorbent at protonated surface sites.

- **Effect of pH on fluoride adsorption capacity**

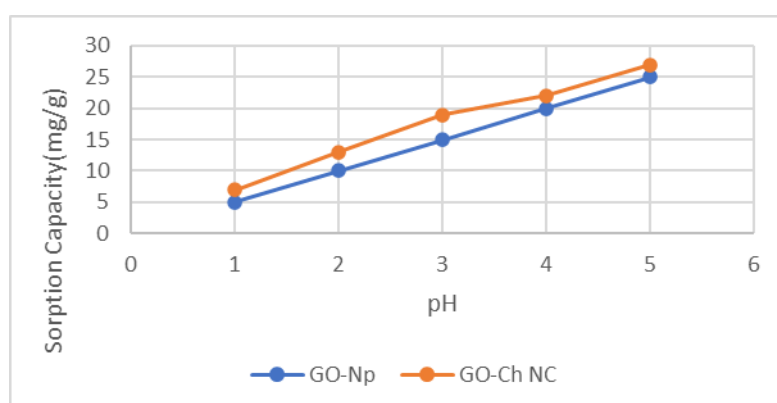


Figure 9. Absorption capacity of GO and GO-Ch NC at different pH

At several pH ranges, synthesised adsorbents were tested for fluoride removal. Figure 8. demonstrates pH-dependent adsorbent adsorption capacity. At pH 1, fluoride elimination reduced, but at pH 5, it increased. At low pH, GO and GO-Ch NC nanoparticles' protonated amine, carboxylic acid group, and higher potential

metal ion increased adsorption ability. The protonated adsorbent surface sites electrostatically attract negative charge fluoride ions.

- **Effect of Temperature on chromium adsorption capacity**

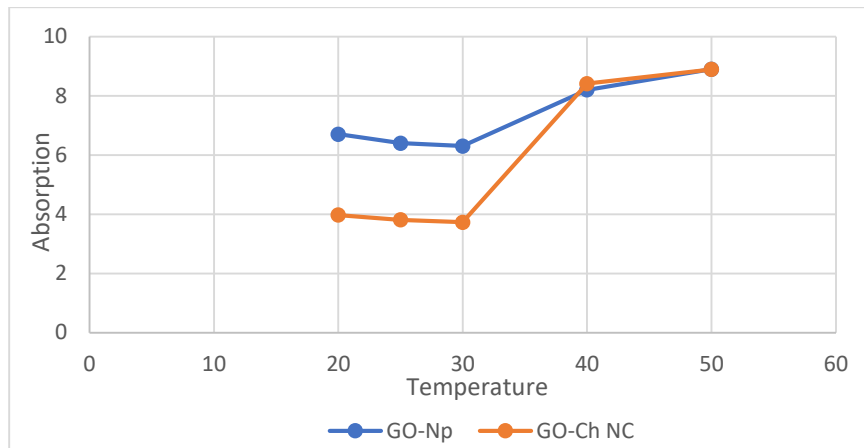


Figure 10. Absorption capacity of GO and GO-Ch NC at different temperatures

The absorption capacity of grapheneoxide nanoparticles and GO-Ch nanocompositewas assessed at a range of temperaturesasshown in figure 10. The temperature at which nanoparticles showed their maximum activitywas 50°C.

- **Effect of Temperature on fluoride adsorption capacity**

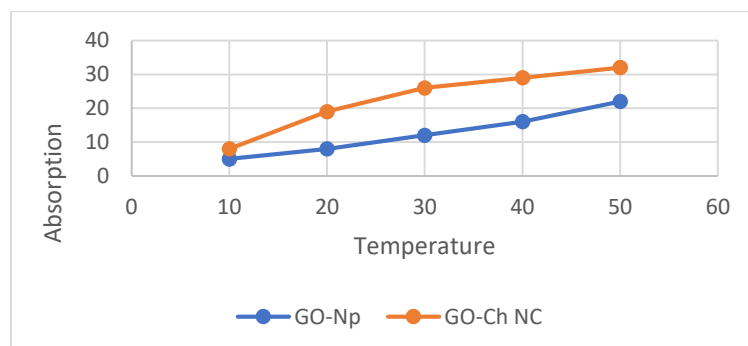


Figure 11. Absorption capacity of GO and GO-Ch NC at different temperatures.

Figure 11. shows graphene oxide nanoparticle and GO-Ch nanocomposite absorption capacities at various temperatures. Nanoparticles were most active at 50°C.

- **Adsorption isotherm**

Cr (VI) and F adsorption isotherms were investigated on GO-Ch-NC to determine the adsorption properties of nanocomposite as it performed better in the batch adsorption study. Changing initial concentrations of fluoride and Cr (VI) from 10 to 100 mg/L was used to perform isotherm experiments. Examining equilibrium adsorption data using Langmuir and Freundlich isotherm models [18-20]. This model assumes a monolayer of active sites with equal energy covers the adsorbent surface. Thus, the optimal adsorption occurs when the

adsorbent reaches a state of total saturation, forming a monolayer that effectively adsorbs fluoride and Cr (VI) ions. The equation presented above serves to demonstrate the underlying paradigm.

$$\frac{c_e}{q_e} = \frac{1}{q_m b} + \frac{1}{q_m} c_e$$

Ce and qe denote the equilibrium adsorbate concentrations in mg/L and the amount adsorbed in mg/g, respectively. The adsorption capacity and energy are determined by the Langmuir constants K_L (L/mg) and q_m (mg/g) (figure 11). Freundlich adsorption isotherm analysis was performed on equilibrium data. This model assumes that heterogeneous surfaces absorb adsorbate molecules. The equation depicts the heterogeneous system with n heterogeneity. Expression of the equation:

The relationship between the quantity of adsorbate adsorbed per unit mass of adsorbent and the equilibrium concentration may be determined by using the equations of the Freundlich isotherm. The Freundlich equilibrium constants, Kf and n, are used in the quantification of the amount of adsorbate adsorbed per unit mass of adsorbent, indicated as qe, as well as the equilibrium concentration, denoted as Ce.

Table 1 displays the Freundlich constant and correlation coefficients (R2) acquired from the graphical depiction of the Freundlich isotherm (see Figure 12). Nanocomposite exhibited advantageous Cr (VI) & fluoride ion due to Freundlich coefficient n meeting criterion $0 < n < 10$. Using correlation coefficients ($R^2 = 0.71$ and 0.81), the Freundlich adsorption isotherm better explains the adsorption of fluoride and Cr (VI) ions. Despite this, Table 1's equilibrium data do not match the Langmuir isotherm model, demonstrating that monolayer adsorption does not occur. Such multilayer and heterogeneous techniques are preferred for Cr (VI) & fluoride ion adsorption.

Table 1. Langmuir isotherm & Freundlich isotherm						
	Langmuir isotherm			Freundlich isotherm		
	qm (mg/g)	KL(L/mg)	R2	Kf(mg/g)(L/mg) ^{1/n}	N	R2
Fluoride	150	1.13	0.77	1.32	1.74	0.81
Chromium (VI)	157	1.15	0.72	1.22	1.76	0.71

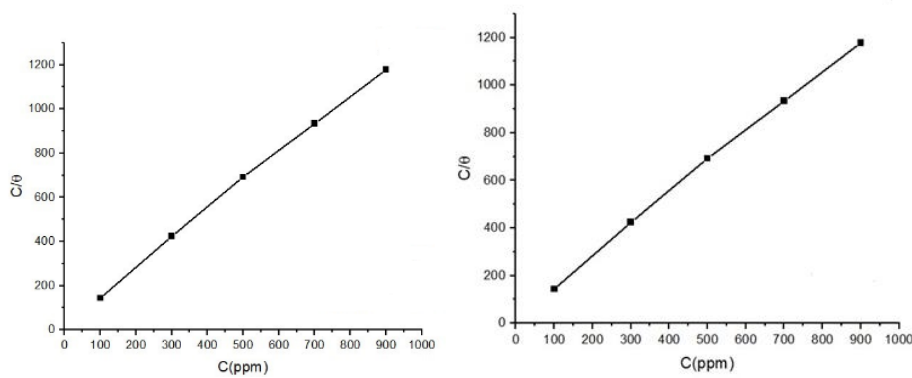


Figure 12. Langmuir isotherm of fluoride and chromium

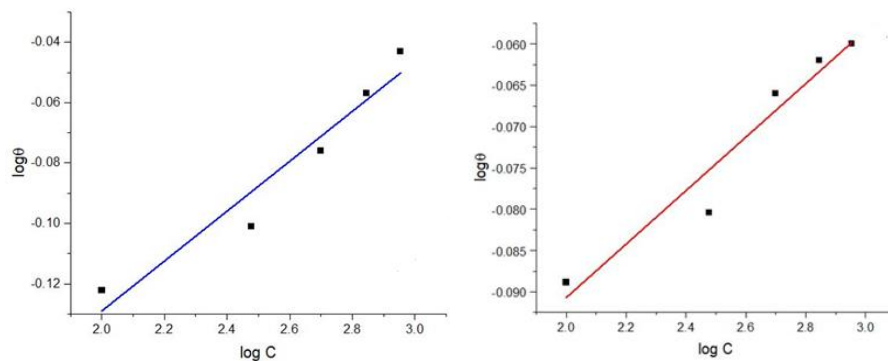


Figure 13. Freundlich isotherm for fluoride and chromium

• Adsorption kinetics

Its capacity to illuminate the chemical routes and processes of adsorption makes adsorption kinetics important. Physical, chemical, and mass transport properties of the adsorbent determine the adsorption mechanism. In order to comprehend GO-Ch-NC adsorption, the kinetics of Cr (VI) and fluoride ion elimination are investigated. Using pseudo-first-order and pseudo-second-order models, the sorption kinetics of Cr (VI) and fluoride ions on GO-Ch-NC were studied. This pseudo-second-order model may be expressed mathematically as follows:

$$\frac{dQ}{dt} = k_2(q_e - q_t)^2$$

Q_e & q_t indicate solute adsorbed on the adsorbent at equilibrium and time t , respectively. The pseudo-second-order equation's rate constant is k_2 [$g / (mg \text{ min})$]. In integral form, the equation is:

$$\frac{t}{q_t} = \frac{1}{k_2 q_e^2} + \frac{1}{q_e} t$$

The slope and intercept of the linear connection between t/q_t & t may determine q_e and k_2 . Table 2 shows a statistically significant linear association between Cr (VI) and fluoride ion elimination on GO-Ch-NC. The strong correlation coefficients between the experimental results and the pseudo-second-order rate law based on adsorption capacity demonstrate the validity of this model.

Table 2. Pseudo-second order for GO-Ch-NC Removal of Cr (VI) & Fluoride Ions			
	k1	R2	qe
Chromium	0.22	0.93	2.33
Fluoride ions	0.95	0.74	3.25

Conclusion

The current study evaluated the adsorption capacity of GO-NP and GO-Ch-NC. XRD, SEM, and FTIR confirmed synthesized nano adsorbents. Batch studies examined the effectiveness of GO-NP and GO-Ch-NC in removing fluoride ions and Cr (VI) from solutions. The adsorption capacity was evaluated by changing the temperature, pH, and adsorbent dosages. At pH 5 and 7, Cr (VI) and fluoride ions were effectively adsorbed. The research found the highest clearance rates for Cr (VI) at 80% and fluoride ions at 55%. For Cr (VI), increasing initial concentrations increased the adsorption percentage. This phenomenon can be attributed to amplification in the quantity of available sites. The results of the isotherm investigations demonstrated the adsorption of Cr (VI) & F onto the surface of GO-Ch-NC as described by the Freundlich isotherm model across all concentrations investigated. This finding suggests adsorption procedure is heterogeneous in nature. Additional research is necessary to investigate the potential of the adsorbent for use in industrial contexts. It is vital to allocate diligent endeavors towards optimizing the process parameters, while also facilitating the seamless transition from laboratory-scale trials to the phase of commercialization.

References

1. Akhtar N, Syakir Ishak MI, Bhawani SA, Umar K. Various natural and anthropogenic factors responsible for water quality degradation: A review. *Water*. 2021 Sep 27;13(19):2660.
2. Jadhav SV, Bringas E, Yadav GD, Rathod VK, Ortiz I, Marathe KV. Arsenic and fluoride contaminated groundwaters: a review of current technologies for contaminants removal. *Journal of environmental management*. 2015 Oct 1; 162:306-25.
3. Morrar R, Arman H, Mousa S. The fourth industrial revolution (Industry 4.0): A social innovation perspective. *Technology innovation management review*. 2017 Nov 1;7(11):12-20.
4. Gill M. Heavy metal stress in plants: a review. *Int J Adv Res*. 2014;2(6):1043-55.
5. Mohan D, Pittman Jr CU. Activated carbons and low-cost adsorbents for remediation of tri- and hexavalent chromium from water. *Journal of hazardous materials*. 2006 Sep 21;137(2):762-811.
6. Keshavarz M, Foroutan R, Papari F, Bulgariu L, Esmaeili H. Synthesis of CaO/Fe₂O₃ nanocomposite as an efficient nano adsorbent for the treatment of wastewater containing Cr (III). *Separation Science and Technology*. 2021 May 24;56(8):1328-41.
7. Kurwadkar S. Occurrence and distribution of organic and inorganic pollutants in groundwater. *Water Environment Research*. 2019 Oct;91(10):1001-8.
8. Lal, S., Singhal, A., & Kumari, P. (2020). Exploring carbonaceous nanomaterials for arsenic and chromium removal from wastewater. *Journal of water process engineering*, 36, 101276.

9. Haldar D, Duarah P, Purkait MK. MOFs for the treatment of arsenic, fluoride, and iron contaminated drinking water: A review. *Chemosphere*. 2020 Jul 1; 251:126388.
10. Joya-Cárdenas DR, Rodríguez-Caicedo JP, Gallegos-Muñoz A, Zanol GA, Caycedo-García MS, Damian-Ascencio CE, Saldaña-Robles A. Graphene-based adsorbents for arsenic, fluoride, and chromium adsorption: synthesis methods review. *Nanomaterials*. 2022 Nov 9;12(22):3942.
11. Karimi-Maleh H, Ayati A, Ghanbari S, Orooji Y, Tanhaei B, Karimi F, Alizadeh M, Rouhi J, Fu L, Sillanpää M. Recent advances in removal techniques of Cr (VI) toxic ion from aqueous solution: A comprehensive review. *Journal of molecular liquids*. 2021 May 1; 329:115062.
12. Xiong JQ, Kurade MB, Jeon BH. Can microalgae remove pharmaceutical contaminants from water? *Trends in biotechnology*. 2018 Jan 1;36(1):30-44.
13. He J, Yang Y, Wu Z, Xie C, Zhang K, Kong L, Liu J. Review of fluoride removal from water environment by adsorption. *Journal of Environmental Chemical Engineering*. 2020 Dec 1;8(6):104516
14. Uppal JS, Zheng Q, Le XC. Arsenic in drinking water—recent examples and updates from Southeast Asia. *Current Opinion in Environmental Science & Health*. 2019 Feb 1; 7:126-35.
15. Nenavath G. Removal of chromium vi and fluoride from wastewater using different techniques.
16. Sahu S, Mallik L, Pahi S, Barik B, Sahu UK, Sillanpää M, Patel RK. Facile synthesis of poly o-toluidine modified lanthanum phosphate nanocomposite as a superior adsorbent for selective fluoride removal: a mechanistic and kinetic study. *Chemosphere*. 2020 Aug 1; 252:126551.
17. Mahapatra A, Mishra BG, Hota G. Studies on electrospun alumina nanofibers for the removal of chromium (VI) and fluoride toxic ions from an aqueous system. *Industrial & Engineering Chemistry Research*. 2013 Jan 30;52(4):1554-61.
18. Talreja N, Kumar D, Verma N. Removal of hexavalent chromium from water using Fe-grown carbon nanofibers containing porous carbon microbeads. *Journal of Water Process Engineering*. 2014 Sep 1; 3:34-45.
19. Maliyekkal SM, Sharma AK, Philip L. Manganese-oxide-coated alumina: a promising sorbent for defluoridation of water. *Water research*. 2006 Nov 1;40(19):3497-506.
20. Tor A. Removal of fluoride from an aqueous solution by using montmorillonite. *Desalination*. 2006 Nov 30;201(1-3):267-76.